Direct Observation of Polytungstate Cluster and Monolayer Tungstate on Zirconium Oxide by High-resolution TEM

Atsushi Satsuma,* Hitoshi Yokoi,† Hiroyuki Nishiyama,† Shiro Kakimoto,† Satoshi Sugaya,† Takafumi Oshima,† and Tadashi Hattori

Department of Applied Chemistry, Graduate School of Engineering, Nagoya University, Furo-cho, Chikusa-ku, Nagoya 464-8603

†*R&D Center, NGK Spark Plug Co. Ltd., 2808, Iwasaki, Komaki, Aichi 485-8510*

(Received July 20, 2004; CL-040845)

Direct observation of WO_3/ZrO_2 by using high-resolution TEM images revealed the formation of polytungstate cluster with a narrow size distribution ranging in 0.4–0.7 nm, and the agglomeration into monolayer tungstate after the aging at 1073 K for 100 h.

From the environmental points of view, replacement of the liquid acid catalyzed process, such as isomerization and alkylation of hydrocarbons, to solid acid catalysis is desired.[1,2] WO_3/ZrO_2 is one of the promising candidates of the key material for "greener" solid acid process.[3–5] Since the first report of the generation of strong acid sites on WO_3/ZrO_2 by Hino and Arata,[6–8] a great deal of attention has been attracted. Since the catalytic performance of WO_3/ZrO_2 strongly depends on the preparation method, tungsten content, and calcination temperatures, many attempts have been carried out on the characterization of supported tungsten oxide on zirconia by means of various physicochemical techniques, i.e., Raman,[9–11] UV–vis,[11,12] XAFS,[12,13] NMR,[14] and so on.[15–17] Aiming the better understanding of the origin of acidity of WO_3/ZrO_2, we examined morphology of surface tungsten oxide on zirconia by high-resolution TEM, and report the first direct observation of polytungstate cluster and layered tungsten oxide on zirconia surface.

ZrO_2 support was prepared by hydrolysis of zirconium oxynitrate 2-hydrate (Kishida, 99%) in distilled water by gradual adding 1.0 mol dm^{-3} an aq NH_4OH solution, filtration of precipitate, washing with distilled water for three times, drying at 383 K, and calcination at 673 K for 24 h. WO_3/ZrO_2 was prepared by impregnation of the obtained ZrO_2 with an aqueous solution of ammonium paratungstate (Mitsuwa) at pH 10 with an aq NH_4OH solution. The suspension was evaporated in rotary-evaporator. The solid thus obtained was dried and then calcined at 973 K for 5 h. The loading of WO_3 was 10 wt %. For the aging treatment, the WO_3/ZrO_2 was heated at 1073 K for 100 h in air. High-resolution TEM images were obtained by a HITACHI HF-2000 at HV = 200 kV. BET surface areas were measured by a flow apparatus according to the one-point method. Raman spectra were measured by a JASCO NRS-1000 spectrophotometer with a laser at 532 nm. XRD diffraction patterns were obtained by a Rigaku RINT-1200 diffract meter using Cu Kα radiation.

In the XRD pattern of WO_3/ZrO_2 before the aging treatment, the lines attributable to tetragonal ZrO_2 phase (ICSD-68589) was observed at $2\theta = 30.3$ degree, together with weaker lines at 28.3 and 31.6 degree, which are assignable to monoclinic ZrO_2 phase (ICSD-15983). The lines attributable to tungsten oxides were not observed in the pattern. In Raman spectrum, the scattering bands attributed to ZrO_2 phase (176, 188, 330, 345, 378, 437, 617, and 637 cm^{-1}) were observed, and also a broad band at 900–1100 cm^{-1} was observed. Since the band at 880 cm^{-1} is assigned to polytungstate,[9,11] and that at 1019 cm^{-1} to symmetic stretching mode of terminal W=O of monotungstate and polytungstate,[10,11] the bands indicate that the surface tungstate is well spread on the zirconia surface. On the other hand, after the aging treatment, a small diffraction line attributable to WO_3 phase was observed at 23.3 degree in the XRD pattern, and the relative intensity of the line of tetragonal phase increased greater than those of monoclinic phase. The relative intensities of the diffraction line of tetragonal phase at 30.4 degree and WO_3 line at 23.3 degree were 29 and 2.1% relative to the monoclinic line at 28.3 degree as 100% after the aging at 1073 K for 100 h. Such structural change was also detected in Raman spectra, i.e., the bands at 804 and 714 cm^{-1}, which are attributable to crystalline WO_3, were observed.

Table 1. BET surface area and W density of 10 wt %WO_3/ZrO_2

Treatment	BET Surface Area /m^2g^{-1}	W Density /nm^{-2}
Before the aging	51.4	5.1
After the aging at 1073 K	30.5	8.5

Table 1 shows BET surface area and W density of the WO_3/ZrO_2 before and after the aging at 1073 K for 100 h. Before the aging, the surface area of WO_3/ZrO_2 was initially 51.4 m^2g^{-1}, and the surface W density was 5.1 W nm^{-2}, which is less than the theoretical monolayer coverage of WO_3, i.e., 7 W nm^{-2}.[11,12] After the aging treatment, the surface area was significantly decreased to 30.5 m^2g^{-1}. As a result, the surface W density became 8.5 W nm^{-2} and exceeded the theoretical monolayer coverage. As Iglesia et al. reported,[11] the most essential determining factor of the supported tungstate structure is the surface W density, and the morphology of surface tungstate significantly changes around the theoretical monolayer coverage (W density of 4–8 W nm^{-2}). Therefore, the detailed structure of the surface tungstate was compared by high-resolution TEM images.

Figure 1 shows high-resolution TEM image of 10 wt %WO_3/ZrO_2 before the aging treatment. The diameters of ZrO_2 particles were around 13–23 nm, which is reasonable value comparing with surface area of 51.4 m^2g^{-1}. Small darker dots, assignable to polytungstate clusters, were observed on the surface of ZrO_2 particles. In the figure, typical clusters were magnified in the upper left corner and pointed by white arrows. The diameters of these clusters are in the range of 0.59 ± 0.16 nm. Interestingly, the cluster size is distributed in very narrow range, although

the sample was prepared by a conventional impregnation method. Considering with the crystallographic parameters of tetragonal WO_3 (ICSD-27962), the diameter of the clusters indicates that these oxide clusters contain 3–5-W atoms. The observed surface coverage by the tungstate clusters was around 32%. Considering the surface W density of 5.1 W nm^{-2}, the theoretical surface coverage of this sample is 73%. Since the ratio of theoretical surface coverage and the observed surface coverage is 2.3, it is reasonable to conclude that around 4-W atoms are agglomerated in these polytungstate clusters.

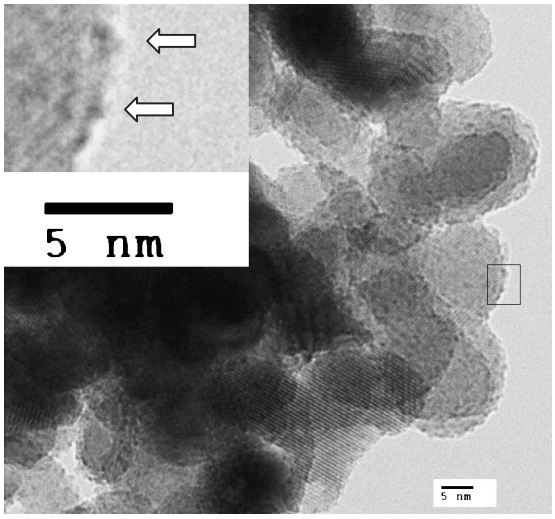

Figure 1. TEM image of 10 wt %WO_3/ZrO_2 before the aging. The enclosed area by square was magnified in the upper left corner.

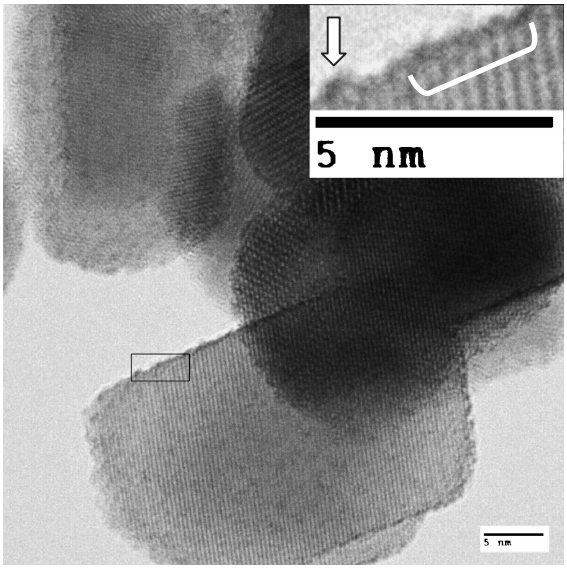

Figure 2. TEM image of 10 wt %WO_3/ZrO_2 after the aging at 1073 K for 100 h in air. The enclosed area by square was magnified in the upper right corner.

Figure 2 shows the TEM images of WO_3/ZrO_2 after the aging at 1073 K for 100 h. The faceted ZrO_2 particles show larger diameter around 31 ± 8 nm. This is in accordance with the decrease in the total surface area to 30.5 $m^2 g^{-1}$, indicating the aging treatment leads to the significant sintering and growth of ZrO_2 particles. Careful observation revealed that polytungstate clusters with ca. 0.6 nm still remained on zirconia surface. As magnified in the upper right corner, the size of a typical polytungstate cluster was 0.76 nm, which is larger but not much agglomerated than those before the aging treatment. Interestingly, as pointed by the white bracket, the surface tungstate in layered form was observed. The presence of layered tungstate indicates that dispersed polytungstate clusters eventually formed W–O–W bonds between neighboring polytungstate clusters, which leads to the formation of 2-D tungsten oxide layer. Although the presence of WO_3 crystallites was suggested by XRD pattern and Raman spectrum, 3-D growth of tungstate was not clarified by the images taken in this study. From the TEM images, at least, it is clear that the three-dimensional growth of tungstate is less significant than sintering of ZrO_2 support.

These high-resolution TEM images clearly revealed the formation of subnano-sized polytungstate cluster on zirconia surface with uniform dispersion before the aging treatment. The correlation between solid acid properties and the nano-structure of surface tunstate is now under the examination and will be reported in near future.

References

1 J. M. Thomas, *Sci. Am.*, **266**, 112 (1992).
2 M. Misono and T. Okuhara, *CHEMTECH*, **23**, 23 (1993).
3 E. Iglesia, D. G. Barton, S. L. Soled, S. Miseo, J. E. Baumgartner, W. E. Gates, G. A. Fuentes, and G. D. Meitzner, *Stud. Surf. Sci. Catal.*, **101**, 533 (1996).
4 G. Larsen, E. Lotero, and R. D. Parra, *Stud. Surf. Sci. Catal.*, **101**, 543 (1996).
5 A. Corma, J. M. Serra, and A. Chica, *Catal. Today*, **81**, 495 (2003).
6 M. Hino and K. Arata, *J. Chem. Soc., Chem. Commun.*, **1988**, 1259.
7 K. Arata and M. Hino, *Proc.-Int. Congr. Catal., 9th*, **1988**, 1727.
8 K. Arata, *Adv. Catal.*, **17**, 165 (1990).
9 D. S. Kim, M. Ostromecki, and I. E. Wachs, *J. Mol. Catal. A: Chem.*, **106**, 93 (1996).
10 S. S. Chan, I. E. Wachs, L. L. Murrell, L. Wang, and W. K. Hall, *J. Phys. Chem.*, **88**, 5831 (1984).
11 D. G. Barton, M. Shtein, R. D. Wilson, S. L. Soled, and E. Iglesia, *J. Phys. Chem. B*, **103**, 630 (1999).
12 D. G. Barton, S. L. Soled, G. D. Meitzner, G. A. Fuentes, and E. Iglesia, *J. Catal.*, **181**, 57 (1999).
13 M. Valigi, D. Gazzoli, I. Pettiti, G. Mattei, S. Colonna, S. De Rossi, and G. Ferrais, *Appl. Catal., A*, **231**, 159 (2002).
14 K. Shimizu, T. N. Venkatraman, and W. Song, *Appl. Catal., A*, **224**, 77 (2002).
15 S. Triwahyono, T. Yamada, and H. Hattori, *Appl. Catal., A*, **242**, 101 (2003).
16 L. M. Petkovic, J. R. Bielenberg, and G. Larsen, *J. Catal.*, **178**, 533 (1998).
17 J. C. Vertuli, J. G. Santiesteban, P. Traverso, N. Cardona-Martinez, C. D. Chang, and S. A. Stevenson, *J. Catal.*, **187**, 131 (1999).

Published on the web (Advance View) August 28, 2004; DOI 10.1246/cl.2004.1250